International Journal of Fluid Machinery and Systems
Vol. 7, No.4, October-December 2014
DOI: http://dx.doi.org/10.5293/IJFMS.2014.7.4.160
ISSN (Online): 1882-9554

Original Paper

A Study on the Fundamental Surge Frequencies in Multi-Stage Axial Flow Compressor Systems

Nobuyuki Yamaguchi

Department of Mechanical Engineering, Meisei University (Retired)
2-1-25, Akanedai, Aoba-ku, Yokohama-shi, Japan, 227-0066
yamaguchi_nandm@tk2.so-net.ne.jp

Abstract

Surge phenomena in multi-stage axial flow compressors were studied with attention to the frequency behaviors. A new parameter "volume-modified reduced surge frequency" was introduced, which took into consideration the essential surge process, i.e., emptying and filling of the working gas in the delivery plenum. The behaviors of the relative surge frequencies at the stall stagnation boundaries, compared with the corresponding duct resonance frequencies, have demonstrated the existence of two types of surges; i.e., a near-resonant surge and a subharmonic surge. The former, which has fundamentally a near-resonance frequency, occurs predominantly at the stall stagnation boundary for the short-and-fat plenum delivery flow-path and the long-and-narrow delivery duct flow-path, and possibly in the intermediate conditions. The latter, which has a subharmonic frequency of the fundamental near-resonant one and occurs mainly in the inter-mediate zone, is considered to be caused by the reduced frequency restricted to a limited range. In relation with those dimensionless frequencies at the stall stagnation boundary, the surge frequency behaviors in more general situations away from the boundaries could be estimated, though very roughly.

Keywords: Fluid Machine, Axial Flow Compressor, Surge, Analytical Simulation, Frequency, Fluid Dynamics

1. Introduction

The fundamental principle of surge phenomena in systems of compressors or pumps has long been understood (for example, Fujii [1], Greitzer [2, 3], etc.). The real surge events, however, are significantly complicated. With the advent of advanced gas turbines, jet engines, combined-cycle plants, industrial compressor plants, etc, being operated at high level of pressure ratios in complicated flow-path conditions, further studies are being demanded for security of the operational safety. In the situations, a number of studies on the detailed behaviors of flows and performance characteristics in surge in the compressor systems have been conducted (for example, Gamache and Greitzer [4], Day, Greitzer and Cumpsty [5], Hosny and Steenken [6], Boyer and O'Brien [7], Copenhaver and Okiishi [8], etc.).

However, it is rather surprising that any generalized information on the surge frequencies and the related features has not necessarily been made clear. It is usually considered that the surge frequencies in compressor surges are related closely with the acoustical resonance frequencies of the air column in the compressor-duct system. According to some examples analyzed by the author (Yamaguchi [9-11]), however, the surge frequencies are not necessarily the same as the resonance frequencies of the system. Possibly, affected by the large amplitude of the surge oscillations and various influential factors, the surge frequencies could deviate much from the acoustical resonance frequencies which assume infinitesimally small perturbations.

The influential factors include a variety of flow-path conditions. For example, geometrical conditions of the flow-path including the compressor and the ductings upstream and downstream, such as duct lengths relative to the dominant acoustical wavelength and changes in the sectional areas, etc., could have effects on the flow conditions. Existence of flow loads, such as large pressure losses in the ducts, heat exchangers, combustors, furnaces, turbines, etc., could affect the phenomena. In long ducts, the pipe frictions could significantly affect both the flow and the acoustics. Exit valve conditions could also affect the phenomena as an important boundary condition for the motion of the whole flow and for the acoustical condition. The

Received February 17 2014; revised June 19 2014; accepted for publication August 5 2014: Review conducted by Prof. Guang Xi. (Paper number O14004C)
Corresponding author: Nobuyuki Yamaguchi, yamaguchi_nandm@tk2.so-net.ne.jp

compressor stalling pressure ratios could also affect the process of emptying and filling the fluid in the delivery duct, which is the essential feature of surges. In multi-stage situations of the compressors, in addition to the global influence by the pressure ratio, stage-wise distributions of working conditions could affect the phenomena, also. For example, differences of working conditions among the stages for far off-design speeds in multi-stage compressors could affect the phenomena (Yamaguchi [11]). Higher harmonic mode surge might happen to occur, though very locally, depending on the duct geometrical conditions and the relative locations of the compressor in the flow-path layout.

This study aims to make clear the basic features of surge frequencies affected by the flow-path geometries and the compressor conditions, in the systems of a multi-stage axial flow compressor and ducts.

For the purpose, first of all, a number of case studies have been conducted to study the effects of the numbers of stages and the compressor speeds on the behaviors of the stall stagnation boundaries in addition to those in the preceding reports (Yamaguchi [9,10]). Next, a new reduced frequency describing the essential surge process is proposed. The behaviors of the surge frequencies at the stall stagnation boundaries are surveyed, from which some features of the surge phenomena at the boundaries are made clearer. Lastly, behaviors of surge frequencies for changing compressor speeds are surveyed in terms of the new reduced frequencies in comparison with those at the stagnation boundary ones.

For the analyses, a surge transient simulation code "SRGTRAN "of own coding (Yamaguchi [12]) was employed.

2. Basic information on the present analyses

2-1 Analysis procedure

The simulation code, SRGTRAN, the details of which can be found in Yamaguchi [12], conducts analyses in space-time coordinate (x, t). The compressor flow-path is made up of a series of control volumes corresponding to respective stages in which equations of conservation of mass, momentum and energy are solved by the two-stage Lax-Wendroff method. The duct flow-paths are divided into a suitable number of control volumes (CVs) in which the method of characteristics is applied. Within the present formulation, it assumes the phenomena only in the axial direction and neglects the effects of circumferential components and the rotating stall phenomena.

Time t is expressed as follows;

$$t = k\Delta t \qquad (1)$$

Here, Δt is the time step determined to satisfy the Courant-Friedrichs-Lewy condition. k means an integer variable indicating time where $k = 0$ means the starting time of the transient analysis.

2-2 A model of the flow-path and the typical sizes

Some basic data about the compressors and the flow-paths are given below for further study on the stall stagnation boundaries and for several case studies concerned with general deep surge behaviors.

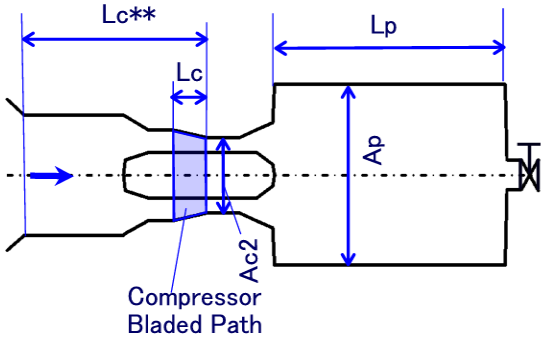

Fig. 1 A modeled flow-path configuration and representative sizes

Table 1 Specifications of the compressors for the analysis and the reference conditions for survey of stall stagnation boundaries

	Comp19	Comp15	Comp13	Comp12	Comp11
Design-condition					
Stages	9	5	3	2	1
rpm	11300	11300	11300	11300	11300
Flow rate (m^3/s)	11.5	11.5	11.5	11.5	11.5
Pressure ratio	3.82				
Reference values					
Tip and hub diameters *Dt, Dh* (m)	0.508 0.356 (Stage 1)	0.508 0.356 (Stage 1)	0.508 0.356 (Stage 1)	0.508 0.356 (Stage 1)	0.508 0.356 (Stage 1)
Area Ac_2 (m^2)	0.04125	0.06057	0.07687	0.08687	0.0975
Length *Lc* ** (m)	4.29	3.978	3.824	3.747	3.67
RPM for analysis (%design speed)	10,000 (88)	10,000 (88)	10,000 (88)	10,000 (88)	15,000- 6000 (133-53)
Stalling Pressure ratio *PR*	3.23	2.05	1.54	1.35	1.444- 1.058
Stage characteristics	Identical for all stages				

Figure 1 shows a schematic model and the representative sizes of the flow-path configuration of the compressor-duct system for the present study. The delivery duct is called here a plenum, including not only a short-and-fat plenum duct but also a long-and-narrow duct. Typical variables concerned are as follows;

Ap, and Lp : sectional area (m^2), and length (m) of the delivery flow-path (plenum), respectively,

Ac_2, and Lc**: exit area of the compressor last stage (m^2), and length (m) of the suction flow-path including the compressor axial length,

u_t: tip speed of the compressor first stage (m/s) as a representative speed.

2-3 Compressors and flow-paths for study

Five compressors were studied in the present study including a single stage compressor, Comp11, and a nine-stage one, Comp19, which have been employed in the previous study (Yamaguchi [9, 10]), and three more ones, Comp12, Comp13, and Comp15 having two, three and five stages, respectively. The respective major quantities are given in **Table 1**. Comp19 is a machine of design speed of 11300 rpm and tip speed of 300 m/s, having a constant-hub annulus configuration designed for a constant stage flow coefficient. Other compressors are derivatives of Comp19. For example, Comp15 employs the first stage through to the fifth stage of those of Comp19.

In the initial phase to study on the flow-path geometries at the stall stagnation boundaries, surge analyses were conducted for two situations. Comp19, Comp15, Comp13, and Comp12 were analyzed for a fixed compressor speed 10000 rpm where front stages were tending to stall and, at the same time, all other stages were in the near-stalling condition. In addition to those, Comp11 of the single stage was analyzed for the speed range of from 15000rpm to 6000 rpm to study the effect of the compressor speed on the surge behaviors where the inter-stage mismatching effects were considered to be negligible. The stalling pressure ratios for respective conditions are given in **Table 1**.

2-4 Stage characteristics of the compressors

Stage characteristics normalized by the tip speed of the first stage u_t as the reference speed is shown in **Fig.2**, which covers a very wide range of flow coefficient from the turbine-action zone to the reversed flow zone, as is required for the kind of simulations. The parameters are given as follows;

Flow coefficient:

$$\phi_t = v_m / u_t \qquad (2)$$

Pressure coefficient:

$$\psi_{Pt} = \frac{C_P T_{T1}\left[\left(P_{T2}/P_{T1}\right)^{\{(\kappa-1)/\kappa\}} - 1\right]}{(1/2)u_t^{\,2}} \qquad (3)$$

Temperature coefficient:

$$\psi_{Tt} = C_P\left(T_{T2} - T_{T1}\right)\Big/(1/2)u_t^{\,2} \qquad (4)$$

Here, v_m: annulus-averaged axial flow velocity, u_t: compressor tip peripheral speed of the first stage (reference speed), P_{T1} and T_{T1}: total pressure and temperature at the stage inlet, respectively, P_{T2} and T_{T2}: total pressure and temperature at the stage exit, respectively, Cp: specific heat at constant pressure, and κ: ratio of specific heats.

The stage characteristics has been supposed on the basis of some literature survey results as described in Yamaguchi [10, 11] particularly in the zones of the stalled flow and the reversed flow where consistent and systematic information are rather few. The identical stage characteristics were employed for all the stages and for all the compressor speeds in the present analyses. Although the procedure might appear somewhat oversimplified in consideration of the significantly variable conditions of both the stage geometries and the flows, it was unavoidable because of lack of suitable estimation methods in the required wide range of the stage working conditions. At the same time, the fixed characteristics could have facilitated examinations about the resulting surge phenomena.

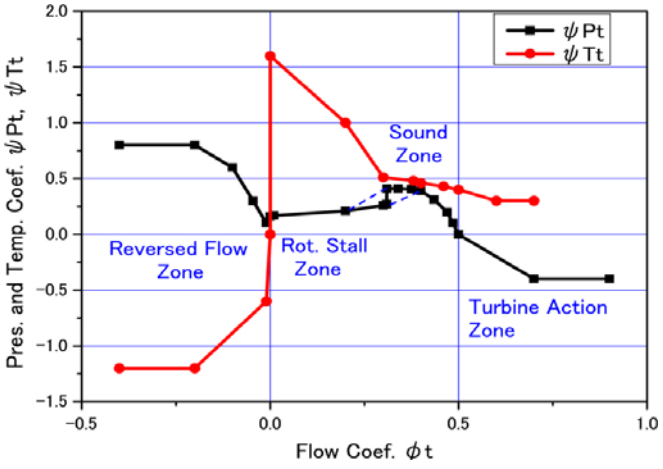

Fig. 2 Wide–range stage characteristics assumed for the compressor stages

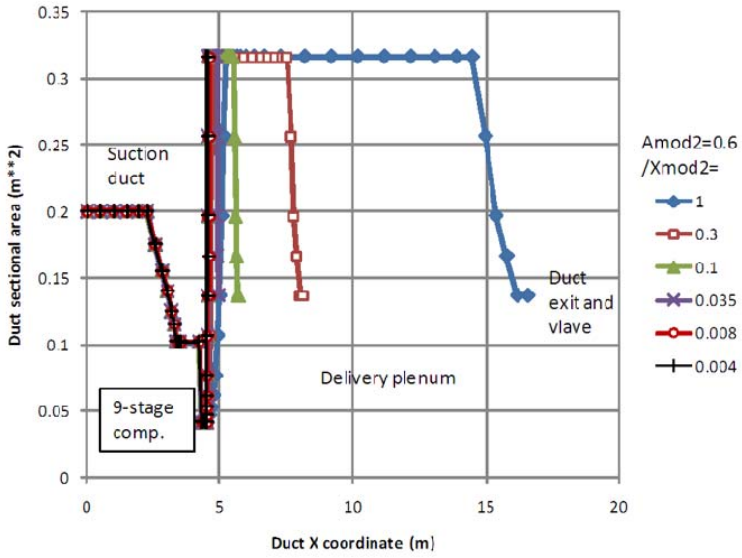

Fig. 3 Some examples of sectional-area distributions along the flowpaths with a given fixed delivery plenum sectional-area.

2-5 Flow-paths for study

Figure 3 shows some examples of the flow-paths for the cases of Comp19. The sectional area of the suction flow -path reduces gradually nearly up to the inlet of the compressor first stage. The delivery flow-path expands downstream of the compressor exit, forming a plenum duct. At the end of the plenum, a short exit pipe was connected and terminated with an exit valve. The present analyses employed fourteen CVs (Control Volumes) for the suction flow-path, a CV for each stage (for example, nine CVs for Comp19), and thirty-four CVs for the delivery flow-path. Other compressors are connected with the suction flow-path identical with that for Comp19 and with delivery flow-paths specified analogously to those of Comp19 in **Fig. 3**.

Geometrical conditions for the stall stagnation boundaries were surveyed at given compressor conditions and speeds by changing the plenum length *Lp* and the sectional area *Ap*, while the suction flow-path configuration were kept the same.

The flow-path configurations were specified by adjusting factors *Amod2* and *Xmod2* applied to a base model.

3. Stall stagnation boundaries

In the first phase, geometrical information on the stall stagnation boundaries is described below. The data are complemented by substitution of additional data on Comp12, 13, and 15 at 10000rpm and Comp11 at 15000-6000rpn to the existing ones on Comp19 and Comp11 at 10000rpm (Yamaguchi [9, 10]).

Figures 4 and **5** show summaries of the flow-path geometries for the stall stagnation boundaries. **Figure 4** shows the normalized geometrical conditions of the boundaries improved from those proposed previously by the author (Yamaguchi [9, 10]), in terms of the following dimensionless quantities.

Sectional area-pressure ratio $APR=(A_P/A_{c2})PR$ (5)

Flow-path length ratio $LR=Lp/Lc^{**}$ (6)

Relative delivery flow-path length: $RLP=Lp/\Lambda$ (7)

Relative suction flow-path length: $RLC=Lc^{**}/\Lambda$ (8)

Here, Λ is the wavelength (m) of the acoustical first-mode resonance frequency f_1 in the system assuming a uniform pressure throughout and the flow temperature distributions just before the compressor stalling. It is related with the average speed of sound a (m/s) in the system and the resonance frequency f_1 as follows;

$$\Lambda=a/f_1 \quad (9)$$

The pipe friction factor λ is given by the following equation;

$$\lambda = \frac{p_L}{(L/D)(1/2)\rho V_a^{\,2}} \quad (10)$$

Here, p_L: pressure loss (Pa), L: pipe length (m), D: pipe diameter (m), ρ: flow density (kg/m^3), V_a: sectional average flow velocity (m/s). The friction factors for the present analyses were set as follows;

$$\lambda = 0.02 \quad (11)$$

Although it is rather large compared with the ordinary level, it is adopted for demonstration of the friction effect on the surge phenomena.

The explanatory note in **Fig. 4**, for example, "19-10000" means Comp19 at 10000 rpm.

The stagnation boundaries in **Fig. 4** are consistent as a whole with the previous ones (Yamaguchi [9, 10]).

Figure 4 shows that deep surges will occur if both of the following two conditions are satisfied; (1) Point (*RLP*, *RLC*) should be located left below the boundary curves in the bottom and, (2) Point (*RLP*, *APR*) should be located above the boundary curves in the top. If both or either of the two points are outside the respective deep-surge zones, stall stagnation will appear.

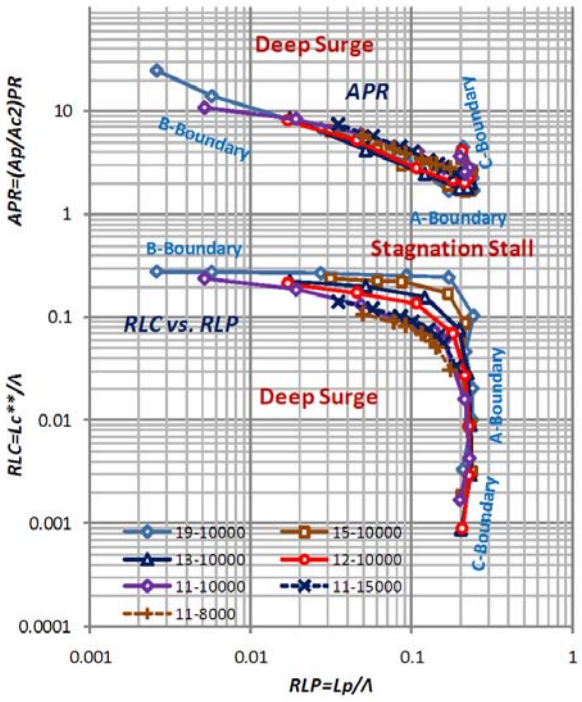

Fig. 4 Geometrical stall-stagnation boundaries and boundary zones

Figure 5 gives the same contents as **Fig. 4,** showing the boundary parameters *APR*, *RLP*, and *RLC* against the flow-path length ratio *LR*. Both figures could be useful respectively in understanding the nature and the situation of the boundaries. It is to be noted that the duct configurations are easier to imagine in the abscissa *LR* in **Fig. 5**. For example, *LR* of unity means that the delivery plenum length *Lp* is equal to the length *Lc*** of the suction duct and the compressor. In **Fig. 5**, the curves of *RLP* and *RLC* appear to give near-mirror images reflected at the length ratio of unity. It suggests changes in the relative importance of the parameters in the respective zones.

In **Figs**. **4** and **5**, the geometrical conditions for the stall stagnation boundaries could be roughly classified into several zones named B, A, C, and B-A transition zone, showing the following respective tendency (Yamaguchi [10]).

B-boundary Zone: *RLC*~0.2-0.3 and very small *RLP* for *LR* < roughly 0.1 (12)

At the same time, a very approximate behavior of *APR* in the zone is expressed as follows;

$$APR \sim 1/\sqrt{RLP} \quad \text{or} \quad APR \sim 1/\sqrt{LR} \tag{13}$$

A-boundary Zone: *RLP*~0.2-0.25 and very small *RLC* for *LR* > roughly 10 (14)

The area–pressure ratio is given very approximately;

$$APR \sim 2\text{-}3 \tag{15}$$

C-boundary Zone: In the presence of significant pipe frictions, the boundary deviates from the A-boundary toward smaller side of *RLP* and larger side of *APR*. In the absence of the pipe friction, only A-boundary zone appears.

It is interesting that the boundary values *Lp* in the A and C zones and *Lc*** in the B zone are approximately a fourth of the resonance wavelength Λ.

In the **B-A transition zone,** or the intermediate zone between the A and B zones, for *LR* below roughly 10 and above roughly 0.1, the boundaries for *RLC* vs. *RLP* are seen in **Fig. 4** to shift gradually their respective locations among those for the single-stage one and the nine-stage one. The tendency appears to depend on the numbers of the stages and the tip speeds, or probably the stalling pressure ratios.

Typical flow-path configurations in the B- and the A-boundary zones are schematically shown in **Figs. 6** and **7**, respectively. In a relative sense, the former could be described as a short-and-fat plenum type delivery flow-path together with a very long suction flow-path, and the latter a long-and-narrow delivery duct together with a very short suction flow-path.

The B-zone is considered to be related with the stagnation condition predicted by a limiting value of the Greitzer's *B* parameter (Greitzer [2, 3]) where the delivery plenum has been approximated as a concentrated volume having negligible axial length.

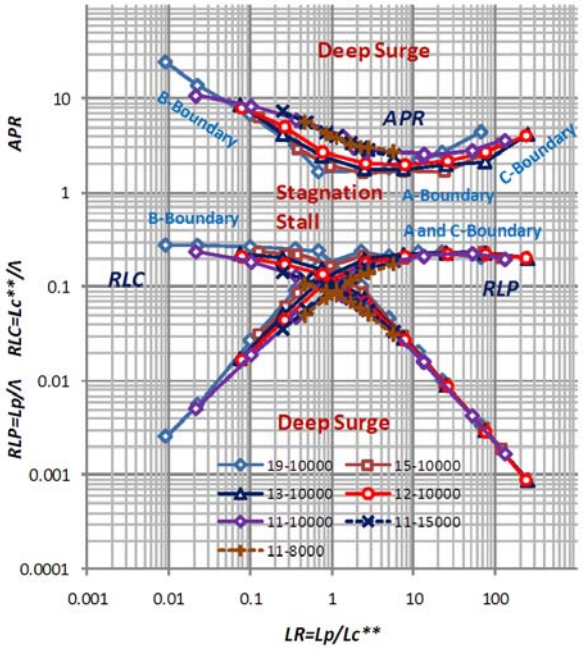

Fig. 5 Behaviors of geometrical stall-stagnation boundaries and boundary zones affected by variable flow-path length ratios

The above geometrical results concerning the stall stagnation boundaries are the starting points for the discussion on the surge frequency phenomena.

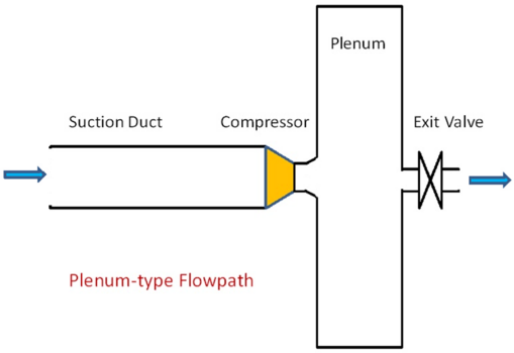

Fig. 6 Qualitative sketch of a very short and fat plenum-type delivery duct near B-type stall stagnation boundary

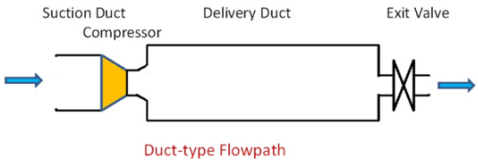

Fig. 7 Qualitative sketch of a long and narrow delivery duct near A- and C-type stall stagnation boundaries

4. Reduced surge frequencies

Surge frequencies could be examined in terms of some reduced frequencies as have often been discussed on flow-related vibrations or oscillations, such as Strouhal numbers for Karman's vortex streets, reduced flutter speeds in flutter vibrations of bodies in flow, etc. Although such trials concerning compressor surge phenomena appear rather few in number, it might be effective in finding out some rules of thumb or summarizing briefly the phenomena in the surge frequencies. The B parameter proposed by Greitzer (Greitzer [2, 3]) is, in a sense, one of such reduced frequencies. Some definite behaviors or limiting values of such reduced frequencies could suggest an essential feature of the concerned phenomena. Here, the author would like to introduce some important surge-related reduced frequencies.

First of all, the reduced surge frequency of ordinary form is defined with respect to the plenum length as below.

$$f_{RPs} = f_{S0} L_P / u_t \tag{16}$$

Here, f_{S0}: deep surge frequency (Hz), and u_t: tip peripheral speed of the compressor first stage (m/s) as a reference of speed.

The above reduced frequency was observed to change much for changing compressor speeds for a particular compressor (Yamaguchi [11]). It is discussed later.

As a next step, in order to describe the essential surge process of emptying and filling of the working fluid in the delivery plenum, a ratio of the following two gas masses is considered.

The mass emptied from or filled into the delivery plenum in one surge cycle with the suction gas density set equal to unity:

$$LpAp[PR^{1/\kappa}\text{-}1] \tag{17}$$

And the mass delivered from the compressor exit into the delivery plenum in one surge cycle:

$$Ac_2 u_t \cdot PR^{(1/k)}/fs_0 \tag{18}$$

Here, PR: stalling pressure ratio. The density ratio is approximated by an isentropic change of the stalling pressure ratio PR. The axial velocity is represented by the tip speed u_t with the flow coefficient omitted. A ratio of the above two quantities gives the following dimensionless parameter f_{RPVVs}.

$$f_{RPVVs} = \frac{f_{S0} A_P L_P (PR^{1/\kappa} - 1)}{A_{C2} u_t PR^{1/k}} = \frac{f_{S0} L_P (1 - PR^{-1/\kappa})}{u_t} \frac{A_P}{A_{C2}} = f_{RPs} \frac{A_P}{A_{C2}} (1 - PR^{-1/\kappa}) \tag{19}$$

It is named here "volume-modified reduced surge frequency", which has a form of the ordinary reduced surge frequency f_{RPs} modified by the ratio of sectional areas and a density-affected term. It is expected to provide a consistent criterion about surge frequencies, which tend to be variable in the changing situations of the flow-path conditions and the compressor operations. It is expected also that the parameter could relate the surge frequencies at the stall stagnation boundaries as the limiting condition with those for changing compressor speeds. In the analytical results about a nine-stage compressor in Yamaguchi [11], the volume-modified reduced surge frequencies had a relatively smaller extent of variations in the values for changing compressor speeds in comparison with those of the simple reduced frequencies defined by Eqs. (16) and (20) below.

In addition to the above, another reduced surge frequency f_{RCs} with respect to the upstream flow-path length Lc^{**} is defined as follows;

$$f_{RCs} = f_{S0} L_C^{**} / u_t \tag{20}$$

The suction-length related reduced surge frequency f_{RCs} is a parameter having a relation with the Greitzer's B parameter (Greitzer [2, 3]).

5. Surge frequencies at the stall stagnation boundaries

In the neighborhood of the geometrical stall stagnation boundary described in **Section 3**, behaviors of the related dimensionless parameters including the volume-modified reduced surge frequency f_{RPVVs} are examined below.

5-1 Volume- modified reduced surge frequency at the stall stagnation boundaries

Figure 8 shows the behaviors of the volume-modified reduced surge frequency f_{RPVVs} against the flow-path length ratio LR. The behaviors are matched with the geometrical conditions at the stall stagnation boundaries shown in **Fig. 5**.

As a global tendency, the boundary behaviors are seen to form upward-sloping curves, consisted of four zones having different characteristics, corresponding to the respective zones shown in **Figs. 4** and **5**. The values of f_{RPVVs} at the stall stagnation boundaries are smaller for short-and-fat plenums in the B-boundary zone, and larger for long-and-narrow delivery ducts in the A- and C-boundary zones. The global trend is related intimately with the behavior of the system resonance frequencies corresponding to the flow-path geometries at the stagnation boundaries.

For LR larger than roughly 7, i.e. in the A-boundary zone, the pipe friction tends to increase the reduced surge frequencies f_{RPVVs} particularly for compressors having nine and five stages, forming the C-boundary region. The smaller delivery area ratios for the higher pressure ratios could have affected the manner. On the other hand, the compressors having fewer stages appear to be influenced little by the pipe

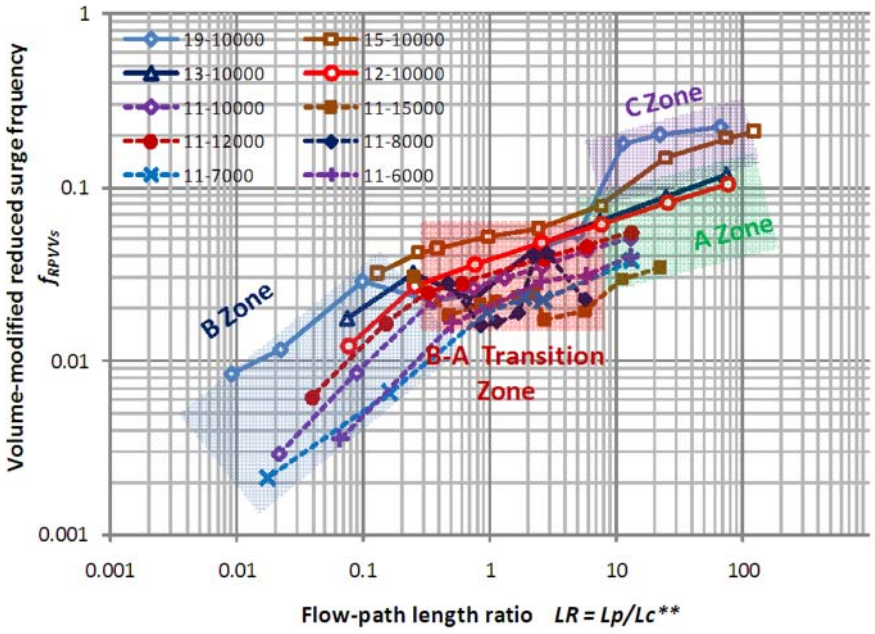

Fig. 8 Behaviors of volume- modified reduced surge frequencies f_{RPVVs} affected by relative flow-path lengths, LR, at the stall stagnation boundaries.

frictions. For frictionless conditions of the flow-paths, not shown here, the C zone vanishes (Yamaguchi [9. 10]).

For *LR* smaller than roughly 0.3, i.e. in the B-boundary zone for the short-and-fat plenum configurations, the effect of the pipe friction is negligible.

In the B zone and the A zone, the values of f_{RPVVs} tend to be larger for larger numbers of compressor stages and higher speeds, i.e., larger stalling pressure ratios, though with some scatters present.

The B-A transition zone from approximately 0.3 to 7 of *LR* is an intermediate zone interfered possibly from both sides. It is to be noted that the reduced frequencies particularly in the zone are seen to have some irregular drops, where the range of the f_{RPVVs} values appears to be limited, as a whole, approximately within from 0.015 to 0.06. The zone is examined in further detail below.

5-2 Relative surge frequencies at the stall stagnation boundaries

Let us watch the phenomena in **Fig. 8** with respect to the surge frequencies at the stall stagnation boundaries. Relative surge frequency, f_{S0}/f_1 is plotted against the flow-path length ratio *LR* in **Fig. 9**. The reference frequency f_1 is the first resonance frequency in the flow-path system estimated by one-dimensional acoustical equations assuming a uniform pressure and the working temperature distribution just before the compressor stalling.

Figure 9 shows slightly-upward-sloping curves running near the horizontal line of f_{S0}/f_1 of unity over the whole range from the B zone to the A zone. They are slightly less than unity in the B zone, increasing to near unity in the A zone and above unity in the C zone, depending on the situations. These frequencies are considered to be driven by the system resonance conditions corresponding to the flow-path geometries at the boundaries. They could be named **near-resonant surges.**

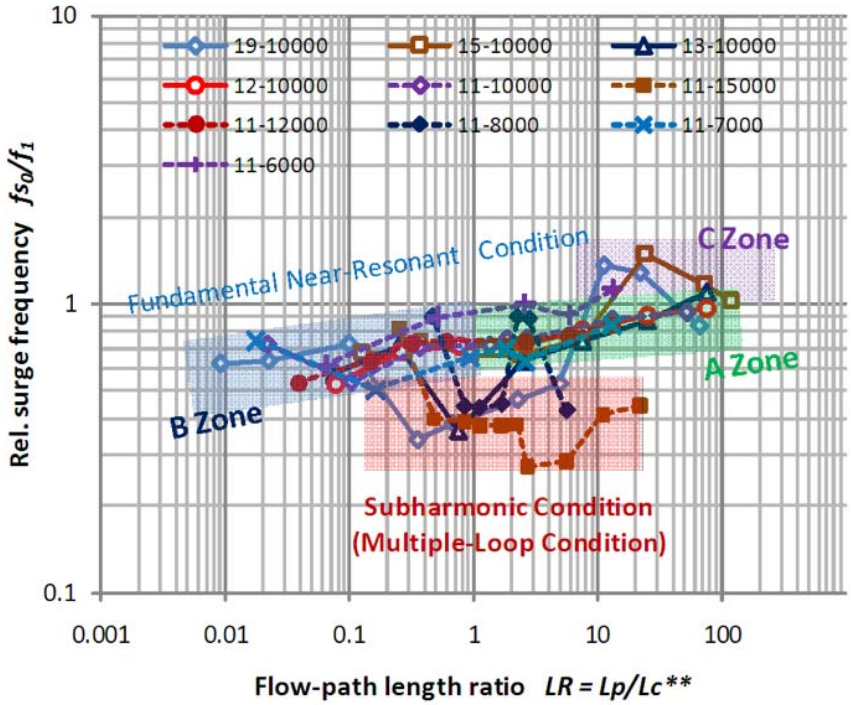

Fig. 9 Behaviors of surge frequencies relative to the respective first resonance frequencies affected by the flow-path length ratios at the stall stagnation boundaries

In addition to those, in the B-A transition zone for *LR* of roughly from 0.1 to 10, appears an isolated zone of reduced level of f_{RPVVs} values covered by the red-color-shaded area of "Subharmonic Condition (Multiple-Loop Condition)". The relative frequencies in the area are between approximately 0.3 and 0.5, which correspond approximately to a third and a second of the above fundamental near-resonant surge ones. These modes could be understood as **(1/3)** and **(1/2) subharmonic surges**, respectively.

The apparently irregular behaviors of the f_{RPVVs} parameter in the B-A transition zone observed in **Fig. 8** are thus understood as a limited range of the values comprising the appearances of the near-resonant surge and the subharmonic surges. The detailed flow conditions involved in the situation are shown in the next section.

The relative frequencies higher than unity seen in the C zone are ascribed to the frictional effects, which tend to constrain the fluid movements, and to reduce the apparent flow-path volumes, causing higher frequencies than expected. The frictional effects have become more significant in the longer-and-narrower delivery flow-path conditions for the stagnation boundaries.

5-3 State of a subharmonic surge

A typical example of the subharmonic surge is shown in **Fig.10** for the condition of Comp11, 15000rpm, *LR of* 2.73, and f_{RPVVs} of 0.01723 near the stall stagnation boundary. Attached numerical figures mean Control Section numbers. Numbers 1 and 50 indicate the inlet and the exit of the whole flow-path, respectively. The compressor exists between 15 and 16, and the delivery plenum between 28 and 46.

Figures 10(a) and **(b)** show time-histories of the pressures and the mass flows, respectively. The sequence after the stalling shows initially a short duration of surge cycles having a higher frequency and a smaller amplitude, and, after that, occurrence of emerging of three or two cycles of the higher-frequency surges. The higher-frequency variations have fundamentally a near-resonance frequency, three repeated cycles of which have formed a complete surge cycle. It means a (1/3) subharmonic surge, including here also temporarily a (1/2) subharmonic surge.

Figure 10(c) shows surge loops described by the pressure versus the mass flow at the compressor exit, demonstrating that one large cycle loop and two small cycle ones make up a complete surge cycle.

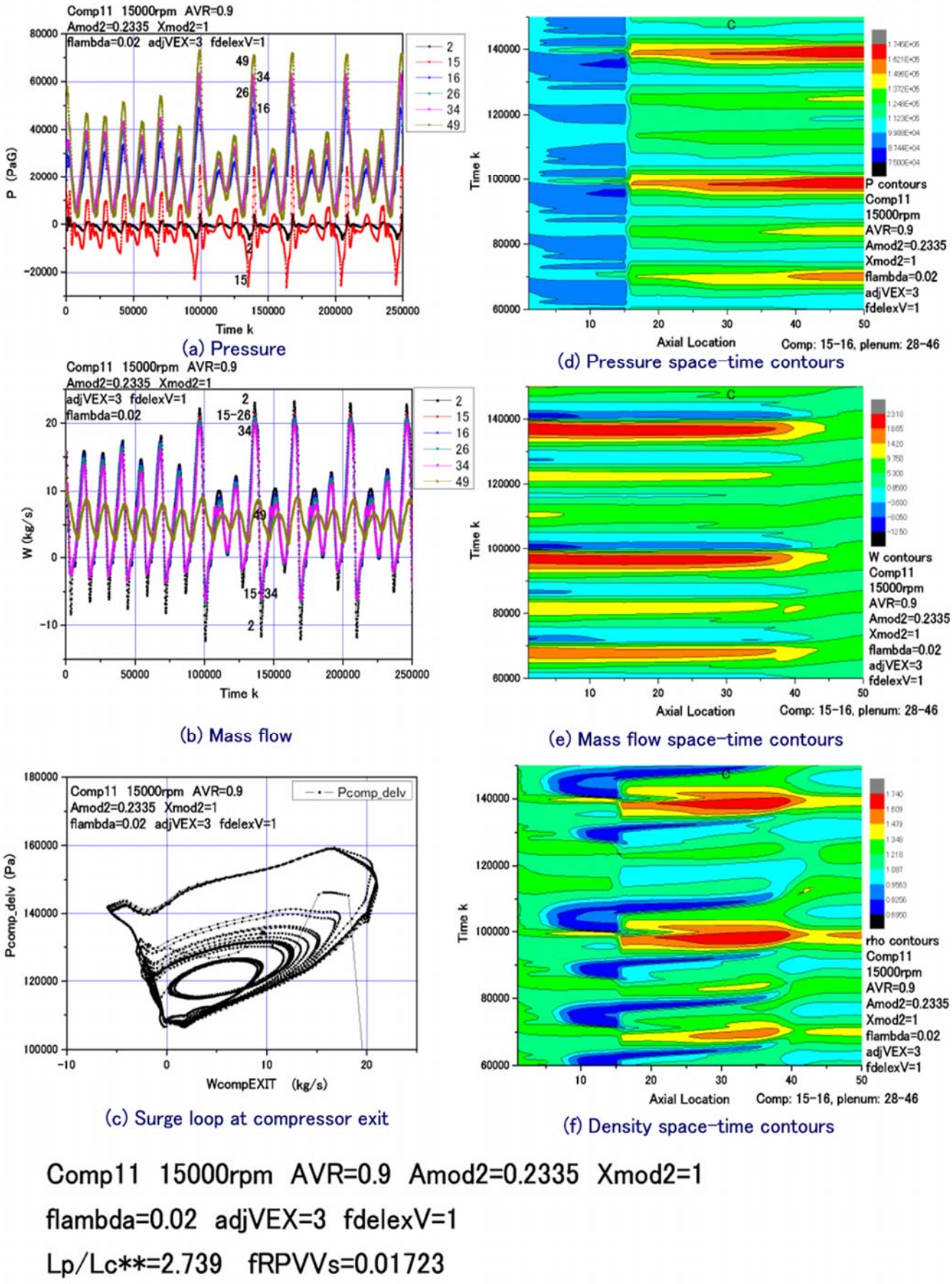

Fig. 10 An example of surge conditions showing a (1/3) subharmonic surge near the stall stagnation boundary for Comp11, 15000rpm, $Lp/Lc^{**} = 2.73$, and $f_{RPVVs} = 0.017233$. $\Delta t = 1.637 \times 10^{-5}$ (s/div). Attached numerical figures indicate Control-Section locations: 1 and 50: the inlet and the exit of the flow-path, 15 and 16: the inlet and exit of the compressor, and 28 and 46: the inlet and the exit of the delivery plenum, respectively.

Figures 10(d-f) show space-time contour maps of the pressures, the mass flows, and the flow densities, respectively, with the flow-path CV number as the horizontal axis and the time k as the vertical axis. The red-colored areas indicate those having the highest values of the quantity in concern and the blue-colored areas the lowest one. The contour maps demonstrate that the subharmonic behaviors are distributed over the whole flow-path, changing locally and temporarily the magnitude and the spread. Particularly, the density contour map in **Fig. 10(f)** shows the changing behaviors clearly. At the same time, it shows that the area of significant density changes is extended as far as upstream of the compressor, not confined within the plenum.

Fundamentally, the appearance of the near-resonant surges in the B zone and the A zone is considered to be triggered by inherently stable and strong effects of the acoustical resonance conditions established in the system. The situation has made the surge frequency stable.

On the other hand, the appearance of the subharmonic surge is considered phenomenologically to be a compromise between two requirements; namely, that the f_{RPVVs} values should be kept within some limited range, roughly 0.015-0.06, and at the same time, that the near-resonant surge frequency should be maintained. In other words, the surge is controlled by the limited range of the reduced frequency f_{RPVVs} values compatible naturally with the essential surge process, i.e., the emptying and filling process, in the coexistence of relatively weak near-resonant conditions. It results in the subharmonic frequencies. The situation could have been realized in the geometrical condition of the comparable order of the flow-path lengths upstream and downstream, i.e., in the B-A transition zone, where the oscillation mode could be relatively flexible.

Mathematically, the large amplitude of the surge oscillations and the resulting nonlinearities in the phenomena could have encouraged the appearance of the subharmonic surge in the zone (for example, Den Hartog [13]).

The subharmonic surges appear not only in the neighborhood of the stall stagnation boundaries as above, but also in the ordinary deep surge situations away from the boundaries. For example, some examples of surge loops and time histories in Figs. 5 through to 8 in Yamaguchi [10] and the phenomena of insufficient surge recovery in a nine-stage compressor in Figs.10(c) and 11(c) in Yamaguchi [11] are considered to be the situations.

5-4 Simple reduced surge frequencies

For reference, **Fig. 11** shows behaviors of the simple reduced surge frequencies f_{RPs} and f_{RCs} at the stall stagnation boundaries, defined by Eqs. (16) and (20). Deep surges occur below the respective curves corresponding to the values of the length ratio LR and the related flow-path geometries given in **Fig. 5**. The following tendencies are observed; In the B zone, f_{RCs} have values of roughly 0.1-0.3, and f_{RPs} are much smaller there. In the A and C zones, f_{RPs} have values of roughly 0.2-0.5, and f_{RCs} are much smaller there. The above values of the simple reduced frequencies give the limiting values in the extreme geometrical conditions for very small values of flow-path length ratios (B zone) or for very large one (A zone) in the stall stagnation situation.

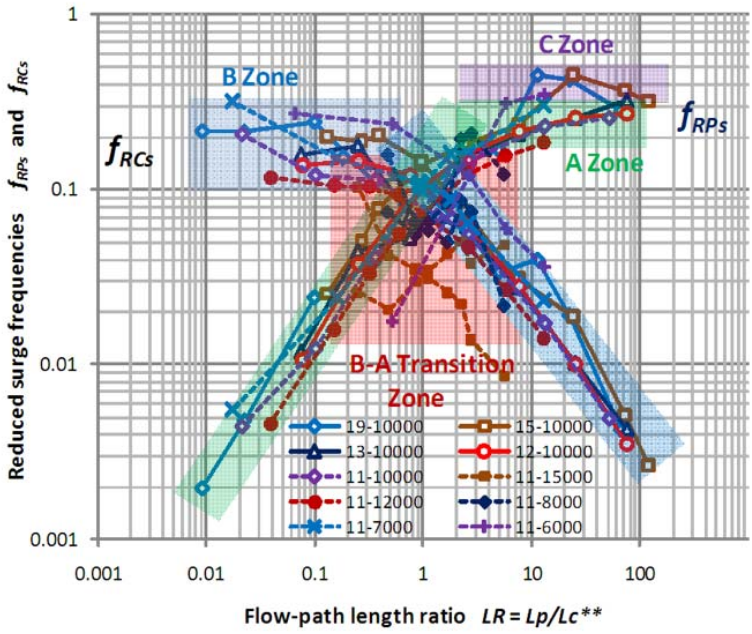

Fig. 11 Simple reduced surge frequencies f_{RPs} and f_{RCs} with respect to the lengths of the delivery plenum flow-path and the suction and compressor flow-path for the stall stagnation conditions

The f_{RCs} values for the B zone and the f_{RPs} values for the A zone are seen to change their positions nearly at the flow-path length ratio of unity. It suggests the relative importance of the local flow-path geometry in the respective zones. In the neighborhood of the length ratio of unity, the reduced frequencies are of comparable orders of magnitude, and their behaviors are seen to be much complicated.

The simple reduced frequency suggests a measure of the time required for the flow to move the local length relative to the surge period. It reflects only the localized situations of the respective flow-paths, which is inconvenient to study on the interactions between the flow-paths upstream and downstream, particularly, in the B-A transition zone.

The reduced frequency f_{RCs} is related, though indirectly, with the Greitzer's B parameter (Greitzer [2, 3]) where the representative frequency is the resonance frequency approximated by that of a Helmholtz resonator in place of the surge frequency. The Greitzer's limiting value of the B parameter of 0.7 - 0.8 for the stall stagnation corresponds very approximately to f_{RCs} of 0.9 - 0.85 in this study. The order of magnitude is comparable with the present results of f_{RCs} for the B zone, which Greitzer has treated.

6. Behaviors in the ordinary deep-surge situations

This section describes about general behaviors of frequencies in the ordinary deep-surge situations having not yet reached at the stall stagnation conditions. Some case studies were conducted where the compressor speeds were lowered from a higher rpm to a near stagnation one for several assumed systems of compressors and flow-path geometries. The results were compared with the stall stagnation boundary data described above in order to show the whole picture of the surge frequency behaviors.

6-1 Data for case studies

Table 2 shows values of the parameters shown schematically in **Fig.1**. The configurations of the delivery flow-path (plenum) were given by specifying values of factors *Amod2* and *Xmod2*, which are adjusting coefficients applied to a basic delivery-duct model to determine the sectional area *Ap* and the length *Lp* of the delivery plenum, respectively. The "short" in the compressor name means a short-and-fat plenum duct condition, where the system tends to approach the B-type stall stagnation when the compressor reduces its speed. The "long" means a long-and-narrow delivery duct where the system approaches the A-type stall stagnation when the compressor reduces its speed. It is to be noted here that for the nine-stage compressor the plenum areas *Ap* are smaller than the compressor exit area A_{C2}, which have been selected in consideration of the area-pressure ratio values near the stall stagnation. The suction flow–paths were kept the same for all cases. The pipe friction factor λ was set equal to 0.02. The compressors are Comp11 of single stage, Comp12 of two stages, and Comp19 of nine stages, designed for 11300 rpm and the reference tip speed u_t of 300.6 (m/s). The compressor speeds were changed to survey the effects on the surge behaviors.

Table 2 The compressors and flow-path configurations for the case studies

Comp	stages	*Amod2*	*Xmod2*	A_{C1}(m^2)	A_{C2}(m^2)	Lc^{**}(m)	*Ap*(m^2)	*Lp*(m)
11-long1	1	0.0312	5	0.10314	0.0975	3.67	0.2231	48.8
11-long2	1	0.6	5	0.10314	0.0975	3.67	0.339	48.8
11-short	1	1.5	0.0582	0.10314	0.0975	3.67	0.7013	0.568
12-long	2	0.2162	30	0.10314	0.08687	3.747	0.1762	292.8
12-short	2	1.0562	0.1	0.10314	0.08687	3.747	0.5232	0.976
19-long	9	-0.0146	10	0.1031	0.04125	4.285	0.03455	97.62
19-short	9	-.043	0.3	0.1031	0.04125	4.285	0.02152	2.928

6-2 Surge frequencies affected by changing compressor speeds

In the respective systems of the compressor and the flow-paths given in **Table 2**, the compressor speeds were changed. In most cases, the exit valve opening areas were set at those for the initial compressor stalling. The deep surge frequency f_{S0} was read from the oscillograms.

The behaviors of the relative surge frequency fso/f_{1x} are shown against the compressor speeds in **Fig. 12**. The reference frequency f_{1x} is the first-mode resonance frequency in the flow-path system specified by the cold-state uniform condition of the suction pressure and the suction temperature throughout. The frequency f_{1x} has a constant value for the changing speeds of the compressor in the identical flow-path configuration.

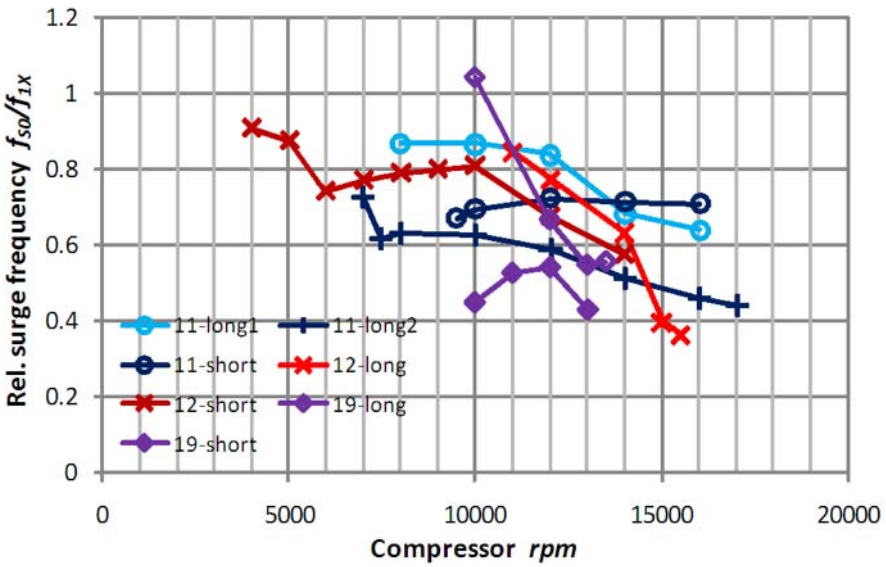

Fig. 12 Some examples of behaviors of relative surge frequencies for changing compressor rpms for combinations of three compressors and various flow-path geometries

The leftmost point of each curve is the point slightly before the stall stagnation in the speed reduction. The stagnations are observed to occur at various compressor speeds, depending on the respective situations of the compressor and the flow-paths.

In **Fig. 12**, the following phenomena are observed;

(1) Generally, the relative surge frequencies, f_{S0}/f_{1x}, are less than unity, namely, the surge frequencies tend to be lower than the

corresponding first resonance frequencies. Within the present analyses, most of the relative frequencies range from 0.9 to 0.35.

(2) For the compressors equipped with long delivery flow paths, the relative frequencies tend to increase for decreasing speeds. For short delivery flow-paths, the relative frequencies tend to increase and then decrease for decreasing speeds.

(3) For the nine-stage compressor equipped with a long delivery duct, a relative frequency happens to be above unity before stall stagnation, which is corresponding to the C-boundary situation affected by the pipe friction. It could be affected also by the changing working conditions of the stages.

(4) In **Fig. 12**, a point of mark + leftward of the kink for "11-long2" and two points of mark × leftward of the kink for "12-short" indicate the conditions extended by throttling further the exit valve, in which the surge frequencies are seen to increase a little.

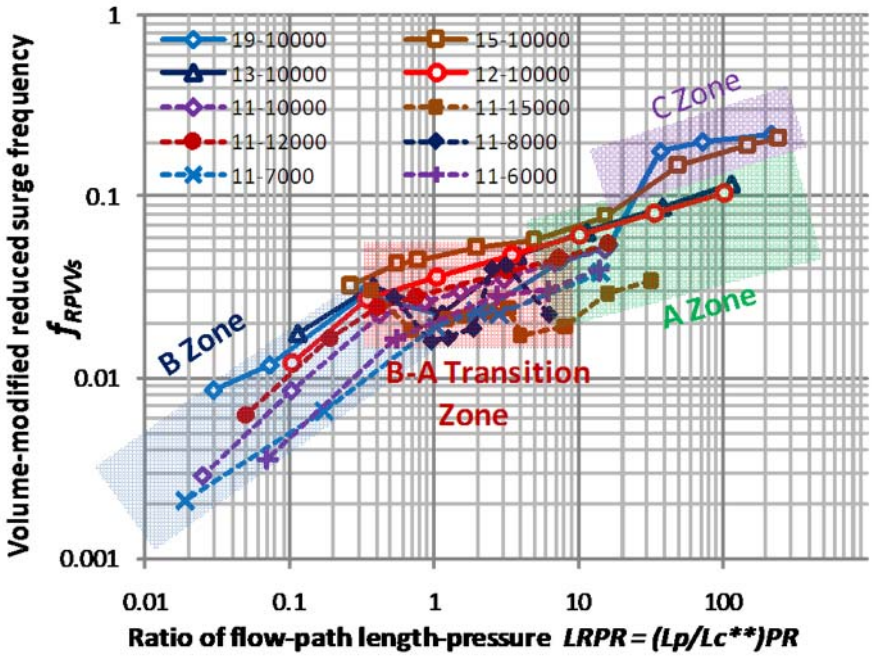

Fig. 13 Behaviors of volume-modified reduced surge frequencies f_{RPVVs} affected by pressure-modified flow-path length ratios *LRPR*

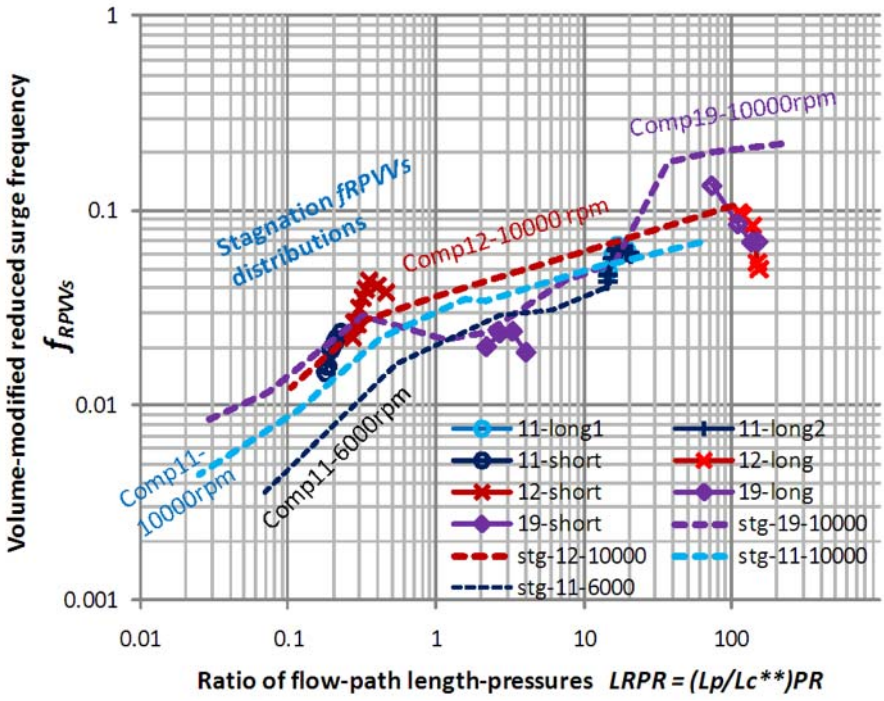

Fig. 14 Some examples of behaviors of surge frequencies in terms of volume-modified reduced surge frequencies f_{RPVVs} affected by pressure-modified flow-path length ratios including the effects of changing compressor rpms for combinations of three compressors and various flow-path geometries, in comparison with those for stall stagnation boundaries

6-3 Variable-speed behaviors of the modified reduced frequency f_{RPVVs}

The above-described frequency behaviors are examined in terms of the volume-modified reduced surge frequency f_{RPVVs} in comparison with those of the stall stagnation boundary data.

Before going further, **Fig. 13** is introduced which is equivalent of **Fig. 8** with its abscissa transferred to the flow-path length-pressure ratio *LRPR*. Here

$$LRPR = LR \cdot PR = (Lp/Lc^{**})PR \qquad (21)$$

It aims to include the effects of compressor speeds in the abscissa only for easier detection of the changes in compressor speeds. By the way, **Fig.13** gives fairly well the f_{RPVVs} behaviors less scattered in comparison with those in **Fig. 8**.

Figure 14 shows the variable-speed behaviors in **Fig. 13** in terms of the volume-modified reduced surge frequency f_{RPVVs} for the case studies in comparison with those at the stall stagnation boundaries in **Fig. 13**. Dotted lines are the stall stagnation boundary data; **blue-colored one for Comp11,10000rpm**, **black-colored one for Comp11, 6000rpm,** **red-colored one for Comp12, 10000 rpm,** and **violet-colored one for Comp19, 10000 rpm.** These lines are typical ones selected from the data shown in **Fig. 13**. Comp11and Comp12 show similar and smooth behaviors over the wide range of *LRPR*, which could be regarded as typical of the effects affected mainly by the system flow-path configurations. Comp19 follows the tendency, on the large, though accompanying some local ups-and-downs in

the B-A transition zone.

Groups of data points connected with solid lines are the case study results on deep surges in variable-speed conditions. A decrease in the compressor speed causes a shift of the data point to the left because of the decrease in the stalling pressure ratio *PR* and in the length-pressure ratio *LRPR*. The variable-speed behaviors of f_{RPVVs} show the following process. For decreasing speeds, and, therefore, decreasing *LRPR*, the f_{RPVVs} points initially in the larger *LRPR* zone tend to increase monotonically, whereas the f_{RPVVs} points initially in the smaller *LRPR* zone tend to increase once and then to decrease nearly along the stagnation boundary line. The left-most points are corresponding to the condition immediately before stall-stagnation in the respective situations. The stagnations occur in the neighborhood of corresponding boundary lines. The behaviors suggest that the variable-speed values of f_{RPVVs} for a fixed geometry system are changeable depending on the compressor speeds, but tend to stay in a narrower range compared with those of the ordinary reduced surge frequencies such as f_{RPs} and f_{RCs} (Yamaguchi [2]).

Thus, the global behaviors of the surge frequencies could be surveyed in terms of the parameter f_{RPVVs} by watching the variable-speed behaviors in the field of the stall stagnation boundaries.

7. A hypothetical model for unification

As is observed in **Fig. 10(f),** the local area of significant density variations during surge cycles is not confined only within the plenum, but could be extended also toward upstream of the compressor. To introduce the effect for more reasonable modelling of the phenomena, it would help to suppose an effective plenum length *Lpeq* including a fraction of the suction flow-path.

For example, though very tentatively, the effective plenum length is assumed as follows;

$$L_{Peq} = L_P + \varepsilon \frac{L_C^{**}}{APR} \tag{22}$$

or

$$L_{Peq} = L_P \left[1 + \varepsilon \Big/ \left\{ \left(\frac{L_P A_P}{L_C^{**} A_{C2}} \right) PR \right\} \right] \tag{23}$$

Here, ε is a coefficient specifying the fraction of the upstream length of possible influence.

Substitution of *Lpeq* for *Lp* in Eq. (17) gives the following formulation of an effective volume-modified reduced surge frequency.

$$f_{RPVVseq} = f_{RPVVs} \left[1 + \varepsilon \Big/ \left\{ \left(\frac{L_P A_P}{L_C^{**} A_{C2}} \right) PR \right\} \right] \tag{24}$$

Figure 15 shows the behavior of $f_{RPVVseq}$ for an assumed coefficient ε of 0.5 against the flow-path length ratio *LR*. The behavior shows a relatively smooth appearance with nearly the same order of slopes from the A zone to the B zone except the B-A transition zone. It suggests that the concept might be qualitatively more probable than **Fig. 8**, though tentative at present.

Outside the B-A transition zone, the surge process are supposed to be controlled by the near-resonant conditions of the effective delivery plenums which are common for both of the B zone and the A zone, including interactions of both flow-paths upstream and downstream.

The B-A transition zone appears to be controlled by a mechanism different from the one described above. It is confined within the following zone;

$$f_{RPVVseq} = 0.018\text{-}0.07 \quad \text{for } LR = 0.3\text{-}7 \tag{25}$$

The above qualitative trial as the first step could be useful to understand the surge phenomena more realistically, although some more

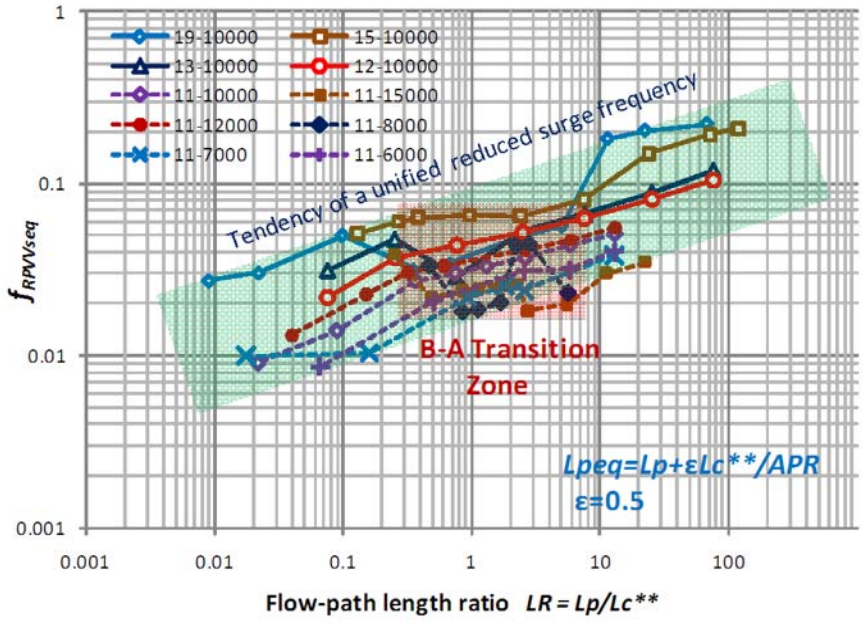

Fig. 15 Behaviors of the effective volume-modified reduced surge frequencies $f_{RPVVseq}$ estimated on the basis of a hypothetical model of the effective plenum length *Lpeq* with ε of 0.5

ingenious models and experimental confirmations would be required.

8. Summary of the basic behaviors of surge frequencies

Basic behaviors and features of the compressor surge frequencies could be summarized as follows on the basis of the above analytical results.

Near the stall stagnation boundaries, two types of surges appear, i.e., near-resonant fundamental surges and subharmonic surges. The near-resonant surge is a fundamental one having a frequency near the acoustical resonance one in the system. It prevails in the B zone and the A zone of the stagnation boundaries, pulled in possibly by a stable and strong mode of the acoustical near-resonance established in the system. On the other hand, the subharmonic surge has a subharmonic frequency of the near-resonant fundamental one. For example, two or three surge cycles, each having a near-resonant surge period and a different amplitude, form a complete surge cycle. It occurs exclusively in the B-A transition zone. The subharmonic frequency is considered to occur in a manner to satisfy a requirement that the values of the volume-modified reduced surge frequency f_{RPVVS} should be kept within a limited range of between 0.015 and 0.06 in the simultaneous existence of a rather weak acoustical resonance condition in the system. The situation could have been realized in the range of the flow-path length ratio *LR* from 0.3 to 7 and for the corresponding geometries for the stall stagnation boundaries, in which the oscillation modes could be changeable rather flexibly.

Similarly, in the general deep surge situations, away from the stall stagnation boundaries, either the near-resonant surge or the sub-harmonic surge occurs. In the variable speed conditions of a specified compressor in a fixed condition of the flow-path geometry, the changing behaviors of surge frequencies are understood in terms of the volume-modified reduced surge frequency tending toward the one in the corresponding stagnation boundary situation.

9. Conclusions

Surge phenomena in multi-stage axial flow compressors were studied, with attention to the frequency behaviors. A new parameter "volume-modified reduced surge frequency" was introduced, which took into consideration the essential surge process, i.e., emptying and filling of the working gas in the delivery plenum. The behaviors of the reduced surge frequency and the relative surge frequency have demonstrated the existence of two types of surges; i.e., a near-resonant surge and a subharmonic surge. The former surge having a near-resonant fundamental frequency occurs predominantly both in the A zone and the B zone, and possibly in the B-A transition zone of the stall stagnation boundary. The latter surge having a subharmonic frequency of the near-resonant fundamental one occurs exclusively in the B-A transition zone.

It is to be noted also that, in practical compressor and flow-path systems, some unexpected behaviors could often be observed, affected possibly by, for examples, local resonances, stage-mismatching effects in multi-stage compressors, some influences from other plant elements, etc. The above results on the basic behaviors could be helpful for further study in such more complicated situations.

It is to be noted further that experimental confirmations are wanted to improve validity of the analytical and numerical research results in the paper.

Symbols

a	Speed of sound (m/s)
Ac_1	Sectional area of the inlet of the compressor first stage (m^2)
Ac_2	Sectional area of the exit of the compressor last stage (m^2)
$Amod2$	Multiplication factor about the sectional area of the delivery plenum
APR	Area –pressure ratio parameter
Av	Valve opening area (m^2)
Avo	Initial valve opening area immediately before steady stalling (m^2)
Cp	Specific heat at constant pressure (J/kg/K)
f_1	The first resonance frequency of an air column (Hz)
f_{1x}	Temporary first resonance frequency of an air column (Hz)
f_{RCs}	Reduced surge frequency with respect to the suction duct
f_{RPs}	Reduced surge frequency with respect to the delivery (plenum) duct
f_{RPVVs}	Volume-modified reduced surge frequency
$f_{RPVVseq}$	Equivalent volume-modified reduced surge frequency
fs_0	Surge frequency (Hz)
Lc^{**}	Length of the compressor-suction flow-path (m)
L_P	Length of the delivery plenum (m)
$Lpeq$	Length of the effective delivery plenum (m)
LR	Ratio of duct lengths
$LRPR$	Ratio of duct length-pressures
PR	Stalling pressure ratio
RLC	Relative length of the compressor- suction flow-path
RLP	Relative length of the delivery (plenum) flow-path
rpm	Compressor revolutions per minute (rpm)
u_t	Referential blade tip peripheral speed (m/s)
V_a	Flow-path section axial velocity(m/s)
v_m	Annulus-averaged axial flow speed (m/s)
x	Axial coordinate along the flow-path (m)

Xmod2	Multiplication factor about the length of the delivery plenum	**Suffix**	
		C	Compressor
ε	Coefficient for equivalent plenum length	P	Plenum
Λ	Wave length for f_1 (m)	R	Reduced condition, ratio, or relative
ρ	Flow density (kg/m^3)	S	Static condition
φ_t	Stage flow coefficient	T	Total condition
ψ_{Pt}	Stage pressure coefficient	s	Surge condition
ψ_{Tt}	Stage temperature coefficient	v	Valve
κ	Ratio of specific heats		
λ	Pipe friction factor		

References

[1] Fujii, S., 1947, Stability and Surging in Centrifugal Pumps, Part 1 and Part 2(in Japanese),” Transaction, Japan Society of Mechanical Engineers Vol. 13, No. 44, pp. 184-191 and 192-201.

[2] Greitzer, E. M., 1976, “Surge and Rotating Stall in Axial Flow Compressors, Part I: Theoretical Compression System Model”, ASME, Journal of Engineering for Power, Vol. 98, pp. 190-198.

[3] Greitzer, E. M., 1976, “Surge and Rotating Stall in Axial Flow Compressors, Part II: Experimental Results and Comparison with Theory”, ASME, Journal of Engineering for Power, Vol. 98, pp. 199-217.

[4] Gamache, R.N. and Greitzer, E.M., 1986, Reverse Flow in Multistage Axial Compressors, AIAA-86-1747.

[5] Day, I.J., Greitzer, E.M., and Cumpsty, N.A., 1978, Prediction of Compressor Performance in Rotating Stall, Journal of Engineering for Power, ASME, Vol. 100, No. 1, pp. 1-14.

[6] Hosny, W.M. and Steenken, W.G., 1986, Aerodynamic Instability of an Advanced High-Pressure-Ratio Compression Component, AIAA-86-1619.

[7] Boyer, K.M. and O’Brien, W.F., 1989, Model Prediction for Improved Recoverability of a Multistage Axial-Flow Compressors, AIAA-89-2687.

[8] Copenhaver, W.W. and Okiishi, T.H., 1989, Rotating Stall Performance and Recoverability of a High-Speed 10-Stage Axial-Flow Compressors, AIAA-89-2684.

[9] Yamaguchi, N., 2012, A Study on the Stagnation-Stall Boundaries Based on Analytically-Evaluated Surge Conditions in Axial Flow Compressors, No. ISUAAAT13-S5-1, The 13-th International Symposium on Unsteady Aerodynamics, Aeroacoustics and Aeroelasticity of Turbomachines.

[10] Yamaguchi, N., 2013, Analytical Study on Stall Stagnation Boundaries in Axial-Flow Compressor and Duct Systems, International Journal of Fluid Machinery and Systems, Vol. 6, No. 2, pp. 56-74.

[11] Yamaguchi, N., 2014, Surge Phenomena Analytically Predicted in a Multi-stage Axial Flow Compressor System in the Reduced-Speed Zone, International Journal of Fluid Machinery and Systems, Vol. 7, No. 3, pp. 110-124.

[12] Yamaguchi, N., 2013, Development of a Simulation Method of Surge Transient Flow Phenomena in a Multistage Axial Flow Compressor and Duct System**,** International Journal of Fluid Machinery and Systems, Vol. 6, No.4, pp. 189-199.

[13] Den Hartog, J.P., 1956, Section 8-10, “*Mechanical Vibrations*”, The fourth edition, McGrawHill Book Co. , (Japanese Edition translated by Taniguchi, O. and Fujii, S., published by Corona Publishing Co., Japan, 1981.